

# Marchantia polymorpha model reveals conserved infection mechanisms in the vascular wilt fungal pathogen *Fusarium oxysporum*

Amey Redkar<sup>1</sup> , Selena Gimenez Ibanez<sup>2</sup> , Mugdha Sabale<sup>1</sup> , Bernd Zechmann<sup>3</sup> , Roberto Solano<sup>2</sup>  and Antonio Di Pietro<sup>1</sup> 

<sup>1</sup>Departamento de Genética, Universidad de Córdoba, Córdoba 14071, Spain; <sup>2</sup>Departamento de Genética Molecular de Plantas, Centro Nacional de Biotecnología CSIC, Campus Universidad Autónoma, Madrid 28049, Spain; <sup>3</sup>Center for Microscopy and Imaging, Baylor University, Waco, TX 76798, USA

Authors for correspondence:

Amey Redkar

Email: ge2rerea@uco.es

Antonio Di Pietro

Email: ge2dipia@uco.es

Received: 20 August 2021

Accepted: 30 November 2021

New Phytologist (2022) 234: 227–241

doi: 10.1111/nph.17909

**Key words:** effectors, endophyte, *Fusarium oxysporum*, *Marchantia polymorpha*, vascular wilt.

## Summary

- Root-infecting vascular fungi cause wilt diseases and provoke devastating losses in hundreds of crops. It is currently unknown how these pathogens evolved and whether they can also infect nonvascular plants, which diverged from vascular plants over 450 million years ago.
- We established a pathosystem between the nonvascular plant *Marchantia polymorpha* (Mp) and the root-infecting vascular wilt fungus *Fusarium oxysporum* (Fo). On angiosperms, Fo exhibits exquisite adaptation to the plant xylem niche as well as host-specific pathogenicity, both of which are conferred by effectors encoded on lineage-specific chromosomes.
- Fo isolates displaying contrasting lifestyles on angiosperms – pathogenic vs endophytic – are able to infect Mp and cause tissue maceration and host cell killing. Using isogenic fungal mutants we define a set of conserved fungal pathogenicity factors, including mitogen activated protein kinases, transcriptional regulators and cell wall remodelling enzymes, that are required for infection of both vascular and nonvascular plants. Markedly, two host-specific effectors and a morphogenetic regulator, which contribute to vascular colonisation and virulence on tomato plants are dispensable on Mp.
- Collectively, these findings suggest that vascular wilt fungi employ conserved infection strategies on nonvascular and vascular plant lineages but also have specific mechanisms to access the vascular niche of angiosperms.

## Introduction

How co-evolution has shaped the interaction between plants and their associated microbes remains a central question in organismic interactions (Bonfante & Genre, 2010; Delaux & Schornack, 2021). Plants have evolved a sophisticated and multilayered immune system to ward off potential microbial invaders (Jones & Dangl, 2006; Boller & Felix, 2009). In addition, pathogens have developed mechanisms allowing them to enter living plants, colonise their tissues and overcome their defence responses. Pathogenicity factors can be either broadly conserved or species specific and include regulators of cell signalling, gene expression or development, as well as secreted effector molecules that modulate the host environment (Jonge *et al.*, 2011; Turrà *et al.*, 2014; Weiberg *et al.*, 2014; Presti *et al.*, 2015; Ryder & Talbot, 2015; van der Does & Rep, 2017).

A particularly destructive group of plant pathogens are those causing vascular wilt diseases, which infect the roots and colonise the highly protected and nutrient poor niche of the xylem (Yadeta & Thomma, 2013). The ascomycete fungus *Fusarium oxysporum* (Fo) represents a species complex with worldwide

distribution that provokes devastating losses in more than 150 different crops (Dean *et al.*, 2012). Fo exhibits a hemibiotrophic lifestyle with an initial biotrophic phase characterised by intercellular growth in the root cortex, followed by invasion of the vasculature and transition to the necrotrophic phase resulting in maceration and death of the colonised host (Redkar *et al.*, 2021). In the soil, Fo is able to locate roots by sensing secreted plant peroxidases via its sex pheromone receptors and the cell wall integrity mitogen activated protein kinase (MAPK) pathway (Turrà *et al.*, 2015). Once inside the root, the fungus secretes a small regulatory peptide that mimics plant Rapid Alkalinisation Factor (RALF) to induce host alkalinisation, which in turn activates a conserved MAPK cascade that promotes plant invasive growth (Masachis *et al.*, 2016). Additional pathogenicity determinants include transcriptional regulators, fungus/plant cell wall remodelling components or secondary metabolites, among others (Michiels & Rep, 2009).

Individual Fo isolates exhibit host-specific pathogenicity, which is determined by lineage-specific (LS) chromosomes that encode distinct repertoires of effectors known as Secreted in Xylem (Six) (Ma *et al.*, 2010; van Dam *et al.*, 2016). Some Six

proteins appear to primarily target plant defence responses, but can also be recognised as avirulence factors by specific host receptors (Houterman *et al.*, 2009; Tintor *et al.*, 2020). In addition to the pathogenic forms, the Fo species complex (FOSC) also includes endophytic isolates such as Fo47, which was isolated from a natural disease suppressive soil (Alabouvette, 1986; Wang *et al.*, 2020). Fo47 colonises plant roots without causing wilt symptoms and functions as a biological control agent against pathogenic Fo strains. How vascular wilt fungi such as Fo gained the ability to associate with plant hosts and evolved endophytic and pathogenic lifestyles remains poorly understood.

The bryophyte *Marchantia polymorpha* (Mp) belongs to the ancient lineage of liverworts and has emerged as the prime nonvascular plant model for studying the evolution of molecular plant–microbe interactions (Evo-MPMI), due to its low genetic redundancy, the simplicity of its gene families and an accessible molecular genetic toolbox (Ishizaki *et al.*, 2008; Lockhart, 2015; Bowman *et al.*, 2017; Upson *et al.*, 2018; Gimenez-Ibanez *et al.*, 2019). Importantly, Mp possesses receptor-like kinases (RLKs), nucleotide binding, leucine-rich repeat receptors (NLRs) and salicylic acid (SA) pathway genes similar to those mediating immune signalling in angiosperms (Xue *et al.*, 2012; Bowman *et al.*, 2017), therefore allowing the study of plant–microbe interactions across evolutionarily distant land plant lineages such as liverworts and eudicots, which diverged >450 million years ago (Ma) (Carella *et al.*, 2018). A current shortcoming of Mp is that only few pathogen infection models have been developed for *in vitro* pathogenicity assays. These include the fungi *Xylaria cubensis* and *Colletotrichum sp1*, the oomycete *Phytophthora palmivora* and the Gram-negative bacterium *Pseudomonas syringae* (Nelson *et al.*, 2018; Carella *et al.*, 2019; Gimenez-Ibanez *et al.*, 2019). A survey of the Mp microbiome identified a number of fungal endophytes, some of which can also act as pathogens (Matsui *et al.*, 2019; Nelson & Shaw, 2019). Whether root-infecting vascular wilt fungi can colonise this land plant lineage, which is evolutionarily distant to eudicots and lacks both true roots and xylem, is currently unknown.

Here we established a new pathosystem between Fo and Mp. We find that Fo isolates that are either endophytic or pathogenic on different crops (tomato, banana, cotton) are all able to colonise and macerate the thallus of this nonvascular plant. Infection of Mp by Fo requires fungal core pathogenicity factors, whereas LS effectors are dispensable suggesting that this vascular wilt fungus employs conserved mechanisms during infection of evolutionarily distant plant lineages. We further show that the fungal transition from biotrophic intercellular growth to necrotrophic maceration and sporulation, which on angiosperms relies on host-specific factors promoting xylem invasion, occurs directly on the nonvascular plant Mp.

## Materials and Methods

### Strains and growth conditions

The tomato pathogenic isolate *F. oxysporum* f.sp. *lycopersici* 4287 (NRRL34936) and its derived mutants, the endophytic

biocontrol isolate Fo47 (NRRL54002), as well as transformants of these strains expressing the GFP derivative mClover3, were used throughout the study (Supporting Information Table S1). In addition, the tomato pathogenic *F. oxysporum* f.sp. *lycopersici* isolate Fol007 and *F. oxysporum* f.sp. *radicis-lycopersici* isolate (NRRL26381), the banana pathogenic isolate *F. oxysporum* f.sp. *cubense* (NRRL54006) and the cotton pathogenic isolate *F. oxysporum* f.sp. *vasinfectum* (NRRL25433) (Delulio *et al.*, 2018) were tested. For microconidia production, fungal strains were grown in potato dextrose broth (PDB) supplemented with the appropriate antibiotic(s) for 3 d at 28°C at 170 rpm. Microconidia were collected by filtration through cheese cloth and centrifugation as described previously (Di Pietro & Roncero, 1998), suspended in sterile water and counted in a Thoma chamber under a Olympus microscope.

### *Marchantia polymorpha* growth conditions and infection assay

Mp accession Takaragaike-1 (Tak-1; male) was used in this study. For *in vitro* assays, Mp gemmae were grown on plates of half Gamborg's B5 medium (liquid medium) at 21°C under a 16 h : 8 h, light : dark cycle. For Fo infections, Mp gemmae were grown for 3 wk on plates of the same medium containing 1% agar and on a Whatman filter paper. Dip inoculation was carried out by immersing the ventral surface of the thalli for 20 min into a suspension of Fo microconidia at the desired concentration in a Petri dish together with the filter paper to cause minimum damage to the thalli. For drop inoculation, a 5- $\mu$ l inoculum with desired spore concentration was applied on the thalli. Mock controls were treated with water. At least three thalli per treatment were used. Filter papers with the inoculated Mp thalli were transferred to a ray-sterilised microbox (Model no. TP1600) fitted with an XXL+ filter (Labconsult, Brussels) containing vermiculite or on solid half Gamborg's B5 medium in Petri dishes and incubated in a growth chamber at 21°C under short-day conditions (10 h : 14 h, light : dark). Disease symptoms were evaluated and imaged at the indicated d post inoculation (dpi). The macerated area on the infected thalli was measured from the central point of the thallus up to the maceration point seen on the apical notch. All infection experiments were performed at least three times with similar results, and representative images are shown.

### Trypan blue staining for visualisation of plant cell death

Trypan blue staining was carried out as described previously (Gimenez-Ibanez *et al.*, 2019) with minor modifications. Briefly, 3-wk-old Mp plants were stained in 0.4% Trypan blue staining solution (Sigma) for 5 min at room temperature. The solution was then replaced with chloral hydrate for destaining (2.5 g of chloral hydrate dissolved in 1 ml of distilled water). Samples were further incubated with shaking for at least 2 d until the tissues were fully destained. Samples were mounted in glycerol for microscopy and images were taken using the Leica DM5000B microscope.

## Tomato root infection assays

Tomato root infection assays were performed as described (Di Pietro & Roncero, 1998). Briefly, roots of 2-wk-old *Solanum lycopersicum* seedlings (cv Monika) were immersed for 30 min in a suspension of  $5 \times 10^6$  microconidia  $\text{ml}^{-1}$  of the different Fo strains and planted in minipots with vermiculite (Projar, Spain). Mock controls were treated with water. In total, 10 plants per treatment were used. Plants were maintained in a growth chamber at 28°C under a 15 h : 9 h, light : dark cycle. Plant survival was recorded daily. Mortality was calculated using the Kaplan–Meier method in GRAPHPAD 9.0 software, USA.

## Scanning electron microscopy

Sample preparation was carried out as reported (Matthaeus *et al.*, 2020) with minor modifications. Small pieces (1 mm<sup>2</sup>) cut from infected Mp thalli at 3 dpi were fixed for 90 min in 2.5% glutaraldehyde in 0.06 M Sorensen phosphate buffer at pH 7.2. After four washes in the same buffer for 10 min each, the samples were dehydrated in a graded series of increasing concentrations of ethanol (50%, 70%, 90%, and 100%) for 20 min per concentration, and critical point dried (Leica EM CPD 300; Leica Microsystems, Wetzlar, Germany) using a customised program for plant leaves with a duration of 80 min (settings for CO<sub>2</sub> inlet: speed = medium & delay = 120 s; settings for exchange: speed = 5 & cycles = 18; settings for gas release: heat = medium & speed = medium). Dried samples were mounted on aluminium stubs with carbon tape, sputter-coated with 10 nm iridium (Leica EM ACE 600; Leica Microsystems) and imaged with a FEI Versa 3D scanning electron microscope (FEI, Hillsboro, OR, USA) under high vacuum conditions.

## Generation of Fol-3x-mClover3 or Fo47-3x-mClover3 tagged *F. oxysporum* strains

A fragment containing three copies in tandem of the *mClover3* gene (Bajar *et al.*, 2016) codon-optimised for Fo (Fo-3x-mClover3) fused to a 3xFLAG tag coding sequence (3xFLAG) was cloned into the pUC57 plasmid backbone under control of the *Aspergillus nidulans gpdA* promoter and the SV40 late polyadenylation signal. Fo-3x-mClover3 labelled strains of Fol4287 and Fo47 were obtained by co-transforming protoplasts with the Fo-3x-mClover3 expression cassette and the hygromycin resistance cassette as described previously (López-Berges *et al.*, 2010).

## Laser scanning confocal microscopy

Laser scanning confocal microscopy was performed using a Zeiss 880 confocal microscope with Airyscan. Mp thalli inoculated with transformants of Fol4287 or Fo47 expressing cytoplasmic 3x-mClover were observed at an excitation of 488 nm and emission detected at 495–540 nm. To visualise plant cell walls, samples were co-stained by incubation in 2 mg  $\text{ml}^{-1}$  propidium iodide (PI) in water for 15 min in the dark as described (Carella

*et al.*, 2019). PI fluorescence was visualised at an excitation of 561 nm, and emission detected at 570–640 nm. Cells were visualised using the bright field differential interference contrast (DIC) channel.

For fluorescein diacetate (FDA) staining, FDA (catalogue no. F7378, Sigma) was dissolved in acetone to a stock concentration of 1 mg  $\text{ml}^{-1}$ . A working solution of 2  $\mu\text{g ml}^{-1}$  was used to stain Mp thalli for testing cell viability of the infected tissue as described previously (Jones *et al.*, 2016). Fluorescein was excited using a 488 nm laser and emission collected between 505 and 530 nm.

## Quantification of fungal biomass *in planta*

For quantification of fungal biomass in tomato roots and stems or in Mp thalli, plant tissue was collected at the desired time points, snap frozen in liquid N<sub>2</sub> and finely ground to powder in a bead beater. Genomic DNA (gDNA) was extracted using a modified chloroform: octanol extraction protocol (Torres *et al.*, 1993) and used for quantification of fungal biomass using real-time quantitative polymerase chain reaction (RT-qPCR). Cycling conditions were 10 min at 95°C followed by 40 cycles of 10 s at 95°C, 10 s at 62°C or 64°C depending on the primer pair used, and 20 s at 72°C. Data were analysed using the  $\Delta\Delta C_t$  method (Livak & Schmittgen, 2001) by calculating the ratio of the plant housekeeping genes *SIGadh* (tomato) or *MpEF1a* (Mp) vs the Fol4287-specific *six1* gene (*FOXG\_16418*) or Fo-*actin* (*FOXG\_01569*). Primers used for qPCR analysis are listed in Table S2.

## Preparation of crude fungal extracts

Crude fungal extracts were prepared as described previously (Gimenez-Ibanez *et al.*, 2019). Briefly, Fo cultures were grown in PDB for 3 d at 28°C and 170 rpm. The fungal mycelium was collected by filtration through a cheese cloth, resuspended in water at a ratio of 20–30% (fresh weight/volume), boiled in a water bath for 15 min at 95°C and cooled down to room temperature. The obtained crude extracts containing Fo PAMPs were stored at –20°C and used at an optical density (OD)<sub>600</sub> of 0.2–0.8 to evaluate the effect on Mp growth as described (Gimenez-Ibanez *et al.*, 2019).

## Analysis of gene expression using RT-qPCR

To measure transcript levels of fungal or plant genes in Mp or tomato, total RNA was isolated from snap frozen tissue of three biological replicates and used for RT-qPCR analysis. Briefly, RNA was extracted using TriPure Reagent and treated with DNase (both from Roche). Reverse transcription was carried out with the cDNA Master Universal Transcriptor Mix (Roche), according to the manufacturer's instruction, using 3  $\mu\text{g}$  of total RNA. RT-qPCR was performed using the CFX96 Touch Real-Time PCR Detection System (Bio-Rad). Primers used for RT-qPCR analysis of different plant stress marker genes are listed in Table S2. Data were analysed using the  $\Delta\Delta C_t$  method (Livak &

Schmittgen, 2001) by calculating the relative transcript level of the stress marker genes in relation to that of the housekeeping reference genes Mp*U-box* or Mp*EF1a*. For expression analysis of fungal genes, the Fo-*actin* (FOXG\_01569) or Fo-*peptidyl prolyl isomerase* (FOXG\_08379) were used as references.

For analysis of Mp*CML42*, Mp*WRKY22*, Mp*PR4* and Mp*PR9* gene expression, experiments were performed with RNA extracted from 7-d-old to 14-d-old Mp thalli grown on Gamborg's B5 medium containing 1% agar. Typically, Mp was transferred to liquid Gamborg's B5 medium 2 d before induction with compounds. For chitin treatment, hexaacetylchitohexaose (chitohexaose;  $\beta$ -1,4-D-(GlcNAc)<sub>6</sub>; #O-CHI6) acquired from Megazyme (Wicklow, Ireland) was used at a concentration of 50  $\mu$ M. RNA extraction and clean-up was done using TRIzol reagent (Invitrogen) followed by the High Pure RNA Isolation Kit (Roche) and DNase digestion to remove genomic DNA contamination. First-strand cDNA was synthesised from 1 mg of RNA using the High Capacity cDNA Reverse Transcription Kit (Applied Biosystems, Waltham, MA, USA), according to the manufacturer's instructions. For qPCR, 5  $\mu$ l from one-tenth diluted cDNA was used to amplify selected genes and the housekeeping gene Mp*U-box* using Power SYBR Green PCR Master Mix (Applied Biosystems). Primer sequences are described (Table S2). Quantitative PCR was performed in 96-well optical plates in a 7500 Real-Time PCR System (Applied Biosystems). Data analysis was performed using three technical replicates from one biological sample. Error bars represent standard deviation (SD). In all cases, the measurements represent the ratio of expression levels between each sample and controls as indicated in each experiment. All samples were normalised against the housekeeping gene Mp*U-box*. All experiments were performed three times with similar results and representative results are shown.

### Statistical analysis

Statistical analysis was carried out using GRAPHPAD PRISM 9.0 software (San Diego, CA, USA). The statistical test used, number of biological and technical replicates, and the description of error bars are provided in the figure legends.

## Results

### *Fusarium oxysporum* isolates with different angiosperm hosts and lifestyles infect *M. polymorpha*

We first asked whether a root pathogen that is highly adapted to grow in the xylem of angiosperms, such as Fo, can infect a nonvascular plant such as the liverwort Mp. To this aim, thalli of the Mp accession Tak-1 were inoculated by dipping the ventral surface in a suspension of fungal microconidia, an infection protocol commonly used for wilt pathogens. Mp thalli inoculated with the tomato pathogenic isolate Fol4287 exhibited macroscopically visible disease symptoms including chlorosis and progressive maceration of the thallus tissue that were absent in the mock-treated controls and whose severity was dependent on the inoculum

concentration (Figs 1a; S1a). Inoculation with other Fo isolates that infect different angiosperm species such as *F. oxysporum* f.sp. *cubense* (banana), *F. oxysporum* f.sp. *radicis-lycopersici* (tomato roots) and *F. oxysporum* f.sp. *vasinfectum* (cotton) also resulted in similar disease symptoms, including browning and maceration of the central thallus tissue (Fig. S1b). We noted that the symptoms caused by Fol4287, remained mostly localised to the centre of the mature thallus, whereas the meristematic apical notches were less affected and often regenerated after 30–40 dpi (Fig. S2a). A similar pattern of infection has been reported previously for the bacterial pathogen *P. syringae* (Gimenez-Ibanez *et al.*, 2019). To determine whether Fo had also colonised the asymptomatic apical thallus regions, we performed microscopy analysis on longitudinal section of the thalli covering both the central and apical areas. This revealed the presence of Fo hyphae in both the macerated and asymptomatic regions (Fig. S2b). The apical thallus regions still contained intact chloroplasts, suggesting that Fo had not entered the necrotrophic phase and did not kill and macerate the host tissue.

We next asked whether a Fo isolate such as Fo47, that displays a strictly endophytic lifestyle on angiosperm hosts (Alabouvette, 1986) is also able to infect Mp. Thalli treated with different inoculum concentrations of Fo47 developed progressive disease symptoms comparable with those of plants inoculated with Fol4287 (Figs 1a; S1a). Although tissue maceration by Fo47 initially progressed more slowly than in Fol4287 (Fig. S1a,b), ultimately similar disease phenotypes were observed at later stages of infection (Fig. 1a). Importantly, the presence of fungal biomass of Fol4287 and Fo47 strains was detected in infected thalli at 6 dpi (Fig. 1c). A drop inoculation method previously described for *P. palmivora* (Carella *et al.*, 2018) resulted in similar symptom development as dip inoculation, although maceration was less severe (Fig. S3a). We conclude that Fo isolates with different host specificities and lifestyles on angiosperms have the ability to infect the nonvascular liverwort Mp.

A comparative scanning electron microscopy (SEM) analysis of the dorsal and ventral surfaces of Mp thalli inoculated with Fol4287 and Fo47 during early infection stages (3 dpi) revealed a similar pattern of hyphal growth on the thallus surface with penetration events located primarily between epidermal cells (Fig. 1d). Occasionally, direct penetration of plant cells by invasive fungal hyphae was also observed. The frequency of penetrating hyphae observed on dorsal and ventral surfaces was between 50–60%, both in the pathogenic and the endophytic *F. oxysporum* strain (Fig. 1d). Confocal microscopy of thalli inoculated either with the tomato pathogenic or the endophytic strain expressing the green fluorescent protein mClover, revealed predominantly intercellular growth of the hyphae (Fig. 1e,f). The pattern of intercellular hyphal penetration and growth of Fo observed in Mp resembled that reported previously for Fol4287 on tomato roots (Pérez-Nadales & Di Pietro, 2011; Redkar *et al.*, 2021). Furthermore, SEM analysis showed Fol4287 and Fo47 hyphae traversing airpores of Mp and growing within the air chambers (Fig. 1g). Although we observed fungal hyphae entangled and coiled around Mp rhizoids, penetration and colonisation of rhizoids was rare and only occurred at the sites of physical damage (Figs 1g; S3b).

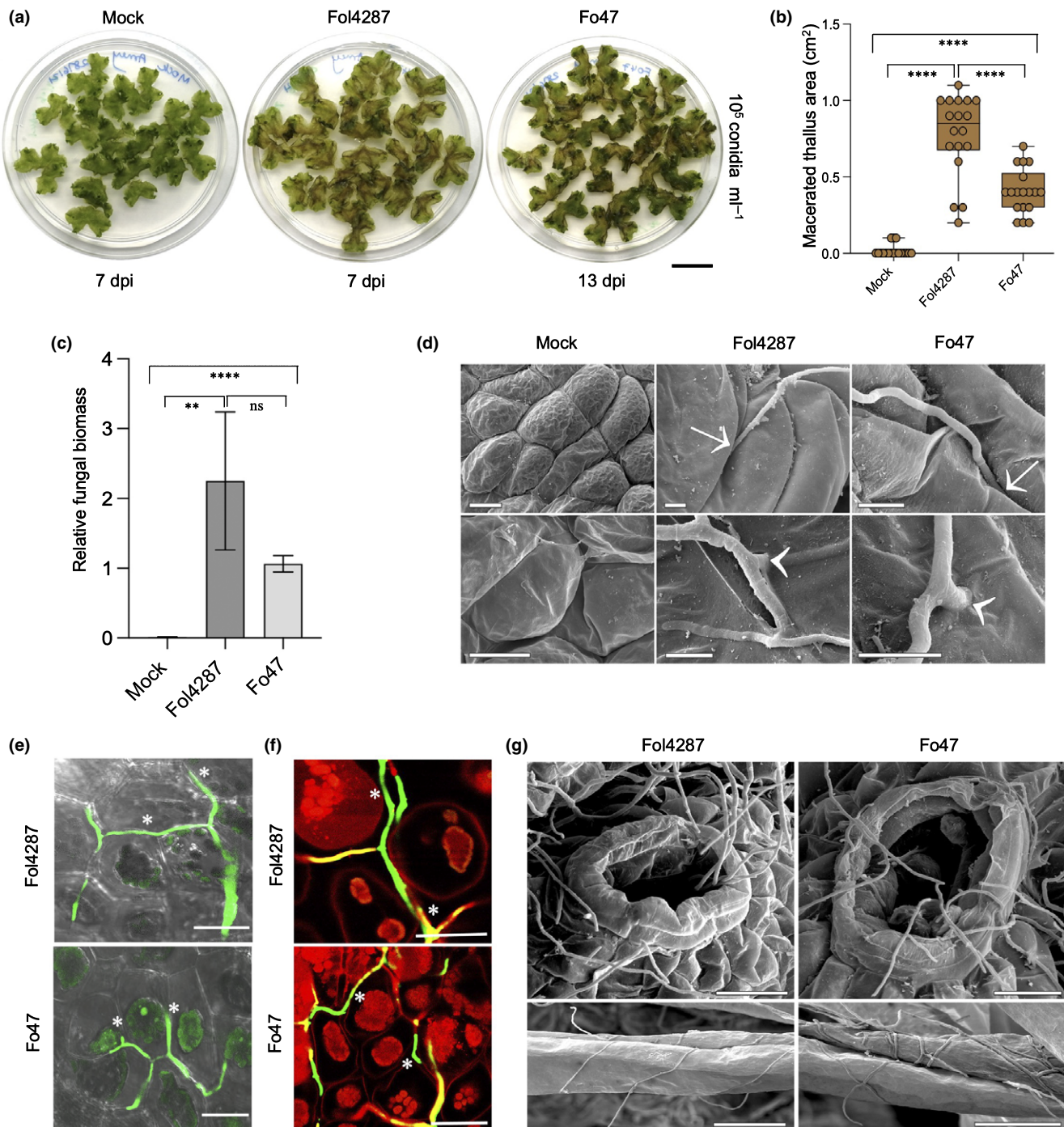


**Fig. 1** *Fusarium oxysporum* strains with different lifestyles infect *Marchantia polymorpha*. (a) Macroscopic images showing disease symptoms on *M. polymorpha* Tak-1 male plants after dip inoculation with  $10^5$  microconidia  $\text{ml}^{-1}$  of the *Fusarium oxysporum* (Fo) strains Fol4287 (tomato pathogen) or Fo47 (endophyte), or water (mock). Images taken at the indicated time points (d post inoculation, dpi) are representative of three independent experiments. Bar, 1 cm. (b) Symptom severity on Tak-1 thalli was measured as the total area of browning at 6 d after inoculation with the indicated Fo strain. Error bars indicate standard deviation (SD) ( $n = 18$  thalli). No browning was observed in the water-treated plants. Asterisks indicate statistical significance (unpaired *t*-test; \*\*\*\*,  $P < 0.0001$ ). (c) Relative fungal biomass on *M. polymorpha* Tak-1 plants 6 d after dip inoculation with the indicated Fo strains or water (mock) was measured by real-time reverse transcription quantitative polymerase chain reaction (RT-qPCR) using primers specific for the Fo-*actin* gene and normalised to the *M. polymorpha* MpEF1a gene. Error bars indicate SD ( $n = 6$ ). Statistical significance was calculated by unpaired *t*-test and indicated by asterisks (\*\*,  $P < 0.01$ ; \*\*\*\*,  $P < 0.0001$ ; ns, nonsignificant,  $P > 0.05$ ). (d) Scanning electron micrographs showing hyphal penetration events on *M. polymorpha* Tak-1 plants 3 d after inoculation with the indicated Fo strain or water (mock). Arrows, intercellular penetration; arrowheads, intracellular penetration. Bar, 20  $\mu\text{m}$  in upper mock image; bar, 5  $\mu\text{m}$  in all other images. (e, f) Confocal microscopy revealing intercellular hyphal growth of the indicated Fo strains expressing mClover on Tak-1 plants at 3 dpi. (f) Samples were stained with propidium iodide (red). Hyphae growing intercellularly *in planta* are indicated with an asterisk. Bar, 25  $\mu\text{m}$ . (g) Scanning electron micrographs showing hyphal growth through the airpores or hyphae entangled on the rhizoids of Tak-1 plants 3 d after inoculation with the indicated Fo strain. Bar, 25  $\mu\text{m}$  in upper images; bar, 50  $\mu\text{m}$  in lower images.

During the initial biotrophic stage on angiosperms, living plant cells adjacent to Fo hyphae remain mostly undamaged (Gordon, 2017). Here, fluorescein diacetate (FDA) staining of Mp thalli during early stages of Fol4287 infection (2 dpi) detected strongly green fluorescent plant cells similar to mock-treated cells (Fig. S4a,b). Active hydrolysis of the fluorogenic ester compound by plant esterases (Saruyama *et al.*, 2013; Jones *et al.*, 2016) indicated that Mp cells remain viable during the early infection stages of Fo. Specificity of the FDA stain for living plant cells was confirmed by including control treatments without the FDA dye as well as a 'dead-tissue' control (10 min at 98°C) before the FDA treatment (Fig. S4a,b). We conclude that early infection and colonisation of the nonvascular plant Mp by Fo occurs mainly via intercellular hyphae in the presence of living Mp cells.

### *Fusarium oxysporum* causes progressive maceration and killing of *M. polymorpha* thallus tissue

During later stages of infection with either Fol4287 or Fo47, Mp thalli exhibited visible signs of tissue maceration and cell killing, suggesting the release of plant cell wall-degrading enzymes by the fungus (Fig. 2a). Previous work established that exopolysaccharonases (exoPGs) and endopolysaccharonases (endoPGs) are secreted by Fol4287 during different stages of tomato plant infection and contribute to fungal virulence (Di Pietro & Roncero, 1998; García-Maceira *et al.*, 2001; Bravo Ruiz *et al.*, 2016). Here we detected a marked upregulation of the transcript levels of *pg1* and *pg5* encoding the two major endoPGs as well as of *pgx6* encoding the major exoPG of *F. oxysporum* during infection of Mp thalli (Fig. 2b). In Fol4287, expression of the two endoPGs increased progressively to reach the highest levels at 3 dpi and then dropped at 7 dpi, while expression of the exoPG followed the same pattern at lower expression levels. These findings reflect a similar trend as reported previously in the angiosperm host tomato (Bravo Ruiz *et al.*, 2016). By contrast, in Fo47 expression of all three PGs was highest at 1 dpi and dropped markedly during later time points. Interestingly, endoPG5 expression in Fol4287 was at least one order of magnitude higher than in Fo47 (Fig. 2b), providing a possible explanation for the slower progression of the maceration process in the endophytic strain Fo47.

To confirm killing of *M. polymorpha* cells by *F. oxysporum*, we performed Trypan blue staining, which revealed the occurrence of cell death in Mp thalli infected with either Fol4287 or Fo47 at 5 dpi, in contrast with the uninoculated control (Fig. 2c). Moreover, microscopy analysis confirmed the presence of blue-stained plant cells showing death signatures (Fig. 2d). In line with this, expression of the Mp cell death marker gene MpTHIO (Mapoly0001s0057) (Gimenez-Ibanez *et al.*, 2019) was upregulated in thallus tissue infected with Fol4287 or Fo47, with transcript levels in Fol4287 approximately twice as high as those in Fo47 at early timepoints (1 and 2 dpi) (Fig. 2e). Collectively, these findings suggested that the tissue collapse and maceration observed in Mp during infection of Fo is associated with secretion of fungal plant cell wall-degrading enzymes such as PGs and

killing of plant cells, probably to ensure nutrient support of the pathogen during host colonisation. Importantly, the necrotrophic phase was accompanied by the production of fungal microconidia and chlamydospores on the macerated thalli tissue compared to the mock-treated sample (Fig. S5a,b). The production of these pathogen structures for dispersal and long-term survival, clearly demonstrated that these Fo strains are able to complete the infection cycle on Mp and therefore act as true pathogens on this non-vascular plant.

### *Marchantia polymorpha* senses *F. oxysporum* molecular patterns to activate the plant defence response

Plants have evolved conserved mechanisms to detect microbial invaders via perception of pathogen-associated molecular patterns (PAMPs) that trigger an efficient immune response (Jones & Dangl, 2006; Boller & Felix, 2009). Here we asked whether Mp can sense molecular patterns from Fo, as previously shown for PAMPs from *P. syringae* (Gimenez-Ibanez *et al.*, 2019). Addition of crude boiled mycelial extracts from Fol4287 or Fo47 to Mp Tak-1 gemmalings grown in liquid medium induced a concentration-dependent growth inhibition (Figs 3a,b; S6). Moreover, in contrast with the mock control, *M. polymorpha* thalli treated with Fo extracts showed rapid upregulation of orthologues of *Arabidopsis thaliana* PAMP responsive genes *WRKY22* (Mapoly0051s0057) and *CML42* (Mapoly0038s0010) (Navarro *et al.*, 2004; Gimenez-Ibanez *et al.*, 2019) (Fig. S6b). These results suggested that crude extracts from Fol4287 and Fo47 contain unknown molecular patterns that trigger a PAMP perception response in Mp.

Next, we asked whether Mp mounts an active defence response during Fo infection, as previously shown for oomycete and bacterial pathogens (Carella *et al.*, 2019; Gimenez-Ibanez *et al.*, 2019). To this aim, the expression of several reporter genes previously described as stress markers was monitored in Mp thalli inoculated with Fol4287 or Fo47 relative to the mock-treated controls. We detected a marked upregulation of MpPAL encoding phenylalanine ammonia lyase that functions in the phenylpropanoid and flavonoid biosynthesis pathways, as well as MpMyb14 encoding a transcription factor involved in the stress response (Kubo *et al.*, 2018) (Fig. 3c). In addition, the expression of two genes encoding pathogenesis-related (PR) proteins that exhibit antimicrobial properties (Ali *et al.*, 2018), MpPR9 (peroxidase) and MpPR4 (chitin binding), was upregulated, although induction of the latter gene was much more pronounced in Fol4287 (Fig. 3c). Also, upregulation of the membrane syntaxin gene MpSYP13B that mediates exocytosis-related cellular changes was specifically detected upon inoculation with Fol4287 (Fig. 3c). Taken together these data suggest that Mp mounts a characteristic defence response during infection by different Fo isolates, and that the response to biocontrol strain Fo47 is less pronounced in comparison to the tomato pathogenic form.

Previous studies revealed that *M. polymorpha* does not respond to flg22, a peptide encompassing a highly conserved domain of bacterial flagellin that acts as a potent elicitor in plants (Gimenez-Ibanez *et al.*, 2019). Here we found that treatment with 50 µM chitohexaose triggered rapid upregulation of

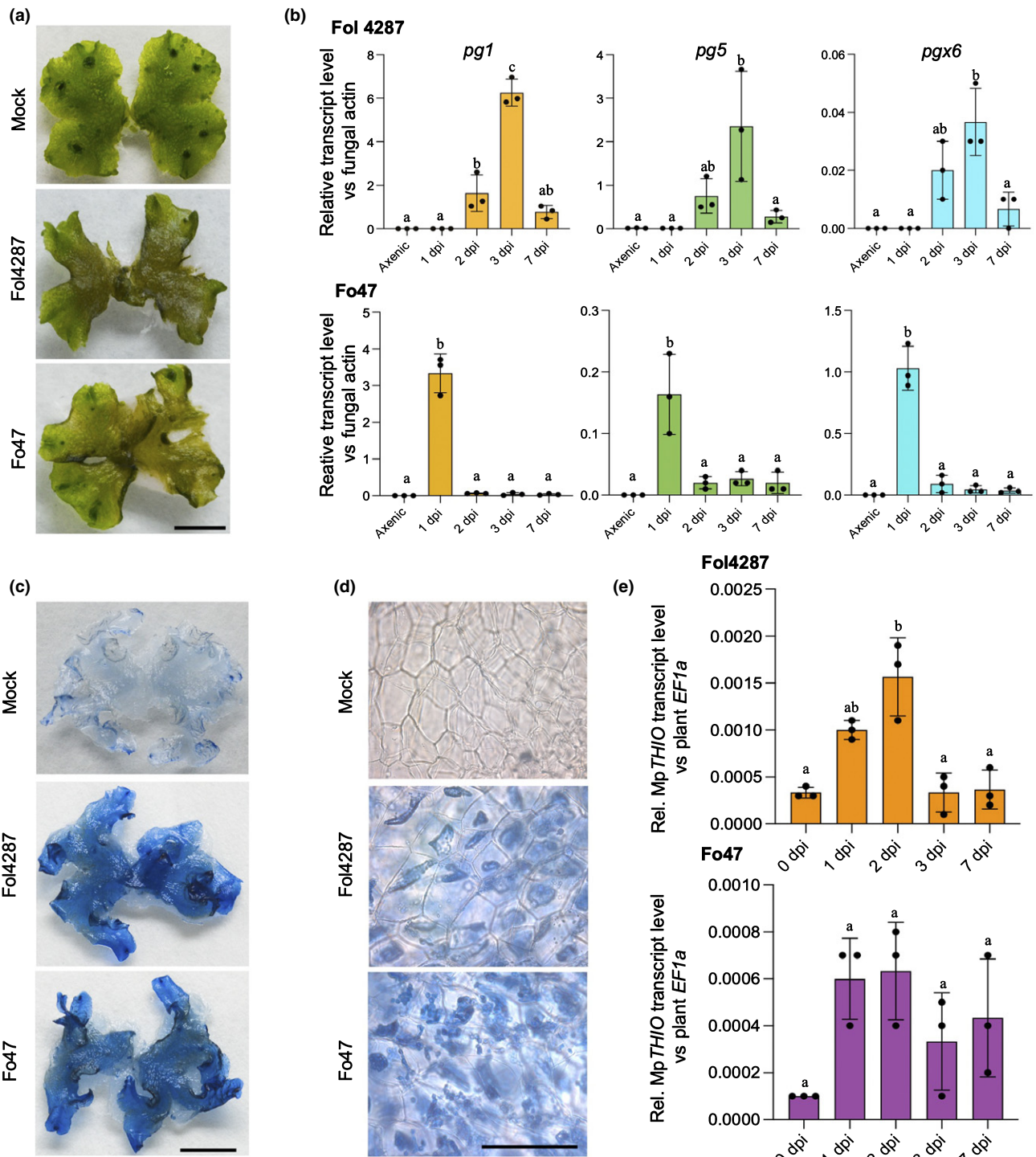


**Fig. 2** *Fusarium oxysporum* (Fo) strains cause maceration and killing of *Marchantia polymorpha* tissue. (a) Macroscopic images showing maceration of thallus tissue in Tak-1 plants 7 d post inoculation (dpi) with  $5 \times 10^6$  microconidia  $\text{ml}^{-1}$  of the indicated Fo strains or water (mock). Bar, 1 cm. (b) Transcript levels of the Fo genes *pg1*, *pg5* and *pgx6* encoding the two major endo-polygalacturonases and the major exo-polygalacturonase, respectively, were measured by reverse transcription quantitative polymerase chain reaction (RT-qPCR) of cDNA obtained from *M. polymorpha* Tak-1 plants at different times after inoculation with the indicated fungal strains or from fungal mycelium grown in liquid minimal medium (axenic). Transcript levels were calculated using the  $\Delta\Delta C_t$  method and normalised to those of the Fo-actin gene. Error bars indicate standard deviation (SD) ( $n = 3$ ). Bars with the same letter are not significantly different according to one-way analysis of variance (ANOVA), Bonferroni's multiple comparison test ( $P < 0.05$ ). (c, d) Macroscopic (c) and microscopic (d) images of Tak-1 plants 5 dpi with  $10^6$  microconidia  $\text{ml}^{-1}$  of the indicated Fo strain or water (mock), stained with Trypan blue to visualise dead plant cells. Images are representative of three independent experiments. Bars: (c) 1 cm; (d) 100  $\mu\text{m}$ . (e) Transcript levels of the *M. polymorpha* cell death marker gene *MpTHIO* were measured in Tak-1 plants at different times after inoculation with the indicated Fo strains as described in (b) and normalised to those of the *MpEF1a* gene. Error bars indicate SD ( $n = 3$ ). Bars with the same letter are not significantly different according to one-way ANOVA, Bonferroni's multiple comparison test ( $P < 0.05$ ).

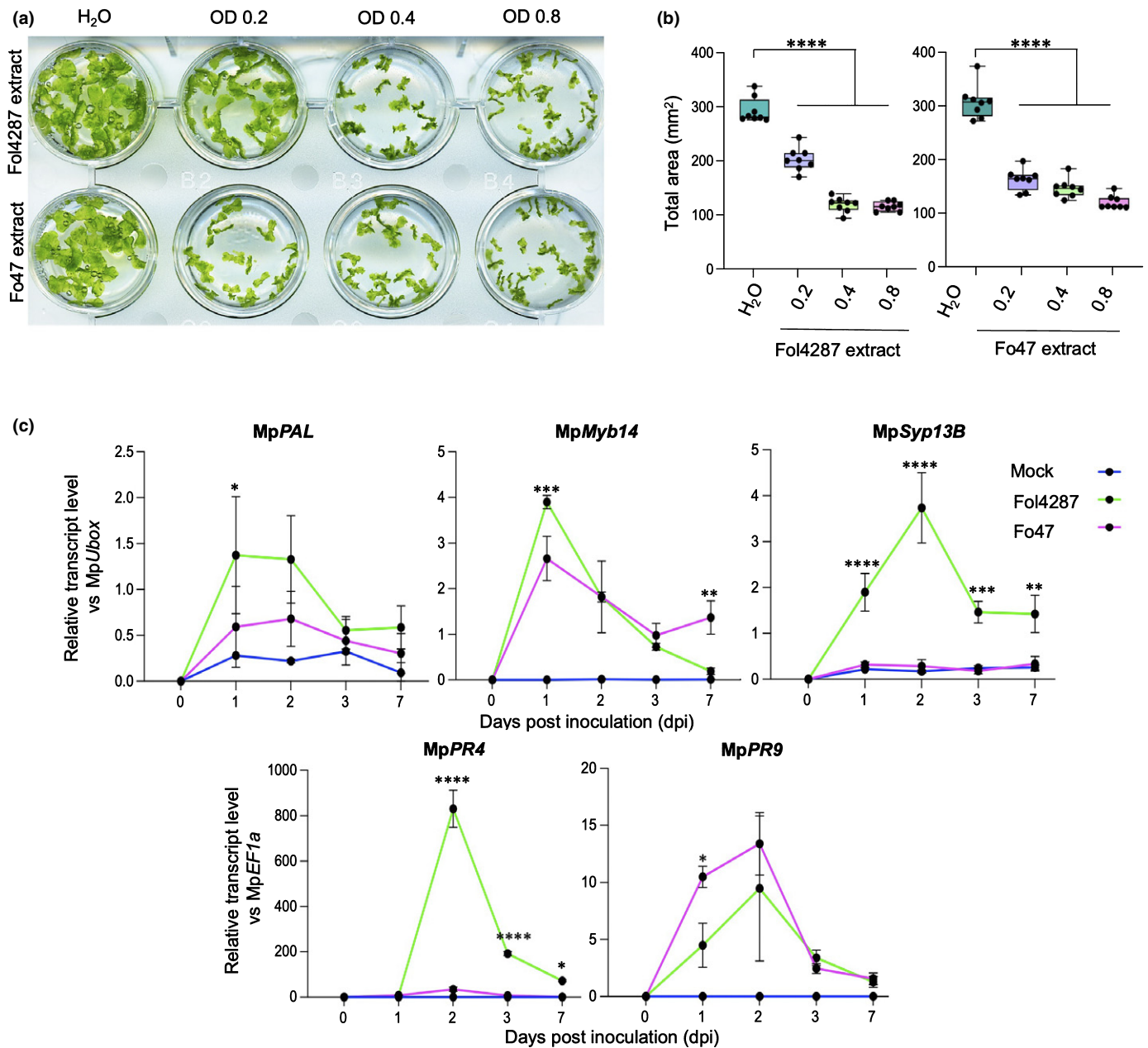


**Fig. 3** *Marchantia polymorpha* senses *Fusarium oxysporum* (Fo) pathogen-associated molecular pattern (PAMP) signatures and induces a defence response. (a, b) Growth inhibition of *M. polymorpha* in response to Fo PAMPs. Tak-1 (male) gemmalings were grown for 14 d in liquid medium containing different concentrations of crude boiled extracts from mycelium of Fol4287 or Fo47 (optical density (OD)<sub>600</sub> = 0.2, 0.4 or 0.8) or water (H<sub>2</sub>O). (a) Images of gemmalings. (b) Quantification of total area (mm<sup>2</sup>) of gemmalings from (a). Error bars represent standard deviation (SD) ( $n = 8$ ). Statistical significance compared with H<sub>2</sub>O-treated plants is indicated by asterisks (\*\*\*\*,  $P < 0.0001$ ) according to one-way analysis of variance (ANOVA), Bonferroni's multiple comparison test. (c) *M. polymorpha* mounts a defence response during Fo infection. Transcript levels of plant defence-related genes MpPAL (phenylalanine ammonia lyase), MpMyb14 (transcription factor), MpSyp13B (membrane syntaxin) MpPR4 (chitin-binding protein) and MpPR9 (peroxidase) were measured by reverse transcription quantitative polymerase chain reaction (RT-qPCR) of cDNA obtained from Tak-1 plants 1, 2, 3 and 7 d post inoculation (dpi) with Fol4287, Fo47 or Mock (H<sub>2</sub>O). Transcript levels were calculated using the  $\Delta\Delta C_t$  method and normalised to those of the MpEF1a or MpU-box gene. Error bars indicate SD ( $n = 3$ ). Asterisks indicate statistical significance between Fol4287 and Fo47 (two-way ANOVA, Bonferroni's multiple comparison test; \*,  $P < 0.05$ ; \*\*,  $P < 0.01$ ; \*\*\*,  $P < 0.001$ ; \*\*\*\*,  $P < 0.0001$ ).

MpWRKY22, MpCML42 as well as the PR gene families MpPR4 and MpPR9 (Fig. S6c), which were also induced in response to natural Fo infection. Chitohexaose is derived from chitin, an essential component of the fungal cell wall that acts as PAMP in angiosperms (Shinya *et al.*, 2015). These data suggest that Mp

senses the externally applied fungal PAMP chitohexaose and responds by upregulating orthologues of known PAMP responsive genes from *A. thaliana*, which are also induced in response to crude extracts from different Fo strains. Deciphering how chitohexaose is perceived by Mp will require further work.



Core pathogenicity mechanisms are required for *F. oxysporum* infection on *M. polymorpha*

Fungal phytopathogens have evolved conserved pathogenicity mechanisms that mediate infection of living plant tissue, as well as host-specific effectors that contribute to virulence on a particular host species. Previous studies have identified a number of core pathogenicity factors in Fol4287, including two MAPKs Fmk1 and Mpk1, which control invasive growth and cell wall integrity,

respectively (Di Pietro *et al.*, 2001; Segorbe *et al.*, 2017), as well as the  $\beta$ -1,3-glucanase Gas1 involved in cell wall assembly (Caracuel *et al.*, 2005) or the zinc finger transcription factor Con7-1, which regulates hyphal morphogenesis and infection (Ruiz-Roldán *et al.*, 2015). These factors are essential for infection of tomato plants (Figs 4a,b; S7b), but most of them have no or only minor roles in fungal growth in axenic culture, although the mutants lacking Gas1 or Mpk1 displayed restricted colony growth on solid medium (Fig. S7a), while growing

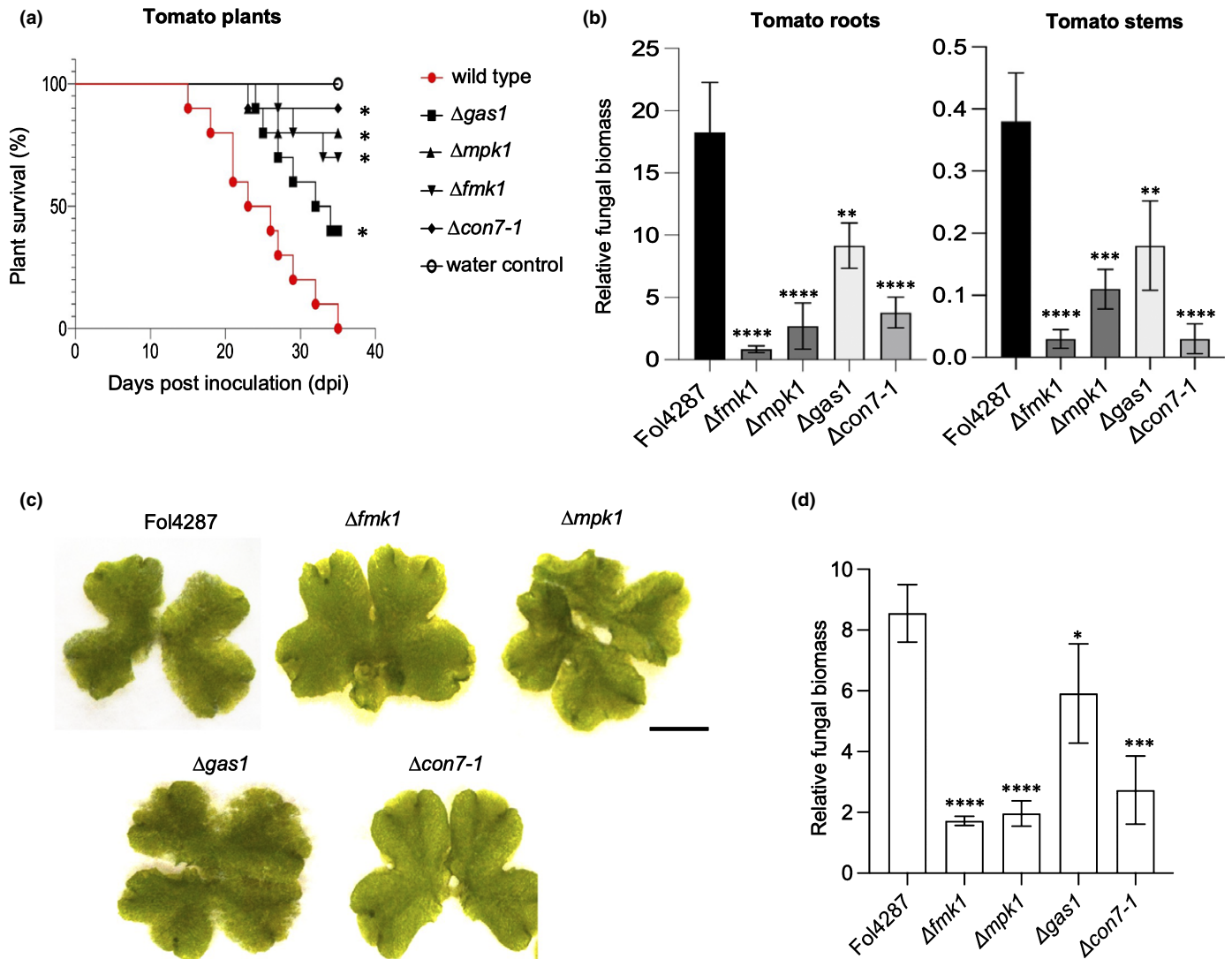


**Fig. 4** Conserved pathogenicity mechanisms drive *Fusarium oxysporum* (Fo) infection on vascular and nonvascular plant hosts. (a) Core pathogenicity genes controlling infection of Fo on tomato plants. Kaplan–Meier plot showing the survival of tomato plants inoculated with the Fol4287 wild-type strain, isogenic mutants in the indicated core genes or water (mock). Number of independent experiments = 3; 10 plants/treatment. Data shown are from one representative experiment; \*,  $P < 0.05$ , vs the wild-type according to log-rank test. (b) Relative fungal biomass in roots or stems of tomato plants 10 d post inoculation (dpi) with the indicated fungal strains was measured by reverse transcription quantitative polymerase chain reaction (RT-qPCR) using primers specific for the Fo4287 *ppi* gene and normalised to the tomato *SI-GADPH* gene. Error bars indicate standard deviation (SD) ( $n = 3$ ). Asterisks indicate statistical significance vs Fol4287 (\*\*,  $P < 0.01$ ; \*\*\*,  $P < 0.001$ ; \*\*\*\*,  $P < 0.0001$ ), according to one-way analysis of variance (ANOVA), Bonferroni’s multiple comparison test. (c) Macroscopic disease symptoms on *Marchantia polymorpha* Tak-1 plants 5 dpi with  $10^5$  microconidia  $ml^{-1}$  of the Fol4287 wild-type strain (wt) or isogenic mutants in the indicated core genes. Images are representative of three independent experiments. Bar, 1 cm. (d) Relative fungal biomass on *M. polymorpha* Tak-1 plants 6 dpi with Fol4287 or isogenic mutant strains was measured by real-time RT-qPCR using primers specific for the Fol *six1* gene and normalised to the *M. polymorpha* MpEF1a gene. Error bars indicate SD ( $n = 3$ ). Asterisks indicate statistical significance vs Fol4287 (\*,  $P < 0.05$ ; \*\*\*,  $P < 0.001$ ; \*\*\*\*,  $P < 0.0001$ ), according to one-way ANOVA, Bonferroni’s multiple comparison test.

normally in liquid culture (Caracuel *et al.*, 2005; Segorbe *et al.*, 2017). We found that isogenic  $\Delta fmk1$ ,  $\Delta mpk1$ ,  $\Delta gas1$  and  $\Delta con7-1$  mutants of Fol4287 caused reduced disease symptoms and accumulated significantly less fungal biomass in Mp thalli than the Fol4287 wild-type strain (Fig. 4c,d). Moreover, Trypan blue staining revealed a lower extent of cell death in thalli inoculated with these mutants compared with those inoculated with the wild-type (Fig. S8). Therefore, infection of Fo on a vascular and a nonvascular plant depends on conserved core fungal pathogenicity determinants.

In tomato-infecting Fo isolates such as Fol4287 or Fol007, host-specific pathogenicity is conferred by a suite of Six effectors, which are encoded on the dispensable LS chromosome 14 (Ma *et al.*, 2010). Loss of chromosome 14 impairs virulence on tomato, while deletion of individual effector genes such as *six1* or *six3* genes causes a reduction in virulence (Rep *et al.*, 2004; Houterman *et al.*, 2009; Vlaardingerbroek *et al.*, 2016). Interestingly, expression of *six1* is specifically induced in response to living plant cells (van der Does *et al.*, 2008). Here we detected upregulation of *six1* and *six3* transcript levels in Fol4287 during infection of Mp thalli, although the relative expression levels were three or four orders of magnitude lower than that of those observed during infection of tomato roots (Fig. 5a). Isogenic  $\Delta six1$  and  $\Delta six3$  mutants showed no detectable differences in disease symptom severity caused on Mp Tak-1 thalli compared with the wild-type strain Fol007 (Figs 5b; S9a). Quantification of the fungal burden in  $\Delta six1$  and  $\Delta six3$  mutants showed a slight reduction of *in planta* fungal biomass in the *six1* mutant in contrast with the *six3* mutant, which showed similar levels of colonisation to the wild-type Fol007 (Fig. 5c). This suggests that the Six1 effector may have an accessory role and contribute to Fo colonisation on Mp (Figs 5c; S9a).

In Fol4287, expression of parasitic phase-specific genes is controlled by the transcriptional regulator *SGE1* (*SIX* gene expression 1), which is required for invasive growth within the xylem (Michiels *et al.*, 2009). On Mp thalli, the  $\Delta sge1$  mutant caused similar disease symptoms and accumulated a comparable amount of fungal biomass as the wild-type strain Fol4287, although the pace of symptom development in this mutant was somewhat delayed and more similar to that of the Fo47 strain (Figs 5d,e; S9b). Collectively, these results indicated that the core pathogenicity mechanisms of Fo are conserved between tomato and liverwort, while host-specific effectors or regulators thereof are largely dispensable for infection of Mp.

## Discussion

The availability of the complete genome sequence, a molecular toolset and biotic interaction systems with oomycete and bacterial pathogens (Carella *et al.*, 2018, 2019; Nelson *et al.*, 2018; Gimenez-Ibanez *et al.*, 2019) have made the liverwort Mp the prime model organism for studying plant–pathogen co-evolution across evolutionary timescales (Bowman *et al.*, 2017; Upson *et al.*, 2018; Delaux & Schornack, 2021). Here we established a robust experimental infection protocol in Mp based on the ascomycete fungus Fo, a well characterised and economically

important broad host range fungal pathogen (Dean *et al.*, 2012). To determine disease severity we used measurable parameters such as total area of browning and *in planta* fungal biomass. We used the Mp model to identify conserved pathogenicity mechanisms in this root-infecting wilt fungus that are shared during infection of vascular plants and this nonvascular bryophyte lacking true roots. Furthermore, we compared infection and disease development between different Fo strains displaying either pathogenic or endophytic lifestyles on angiosperm hosts. Importantly, all Fo isolates tested here produced visible maceration symptoms on Mp thalli, regardless of the angiosperm host on which they are known to cause wilting. This finding indicated that the basal ability of Fo to infect a nonvascular host is independent of the host-specific mechanisms conferring vascular adaptation on a given angiosperm species.

The infection cycle of Fo on vascular plants consists of three distinct phases (Fig. 6): Phase I, penetration of the roots and asymptomatic intercellular growth in the root cortex; Phase II, crossing of the endodermis, entry into the xylem vessels and systemic colonisation of the host; and Phase III, extensive maceration of the moribund plant tissue and development of dispersal and resting structures (microconidia and macroconidia, chlamydospores) (Dean *et al.*, 2012). Phases I and III are controlled mainly by core pathogenicity factors (Di Pietro *et al.*, 2001; Caracuel *et al.*, 2005; Pérez-Nadales & Di Pietro, 2011; Ruiz-Roldán *et al.*, 2015; Turrà *et al.*, 2015; Bravo Ruiz *et al.*, 2016; Segorbe *et al.*, 2017), while Phase II depends critically on host-specific effectors that are encoded on dispensable LS chromosomes (Rep *et al.*, 2004; Houterman *et al.*, 2009; Ma *et al.*, 2010; van Dam *et al.*, 2016; Vlaardingerbroek *et al.*, 2016; Tintor *et al.*, 2020). Here we found that Fo is able to infect the nonvascular bryophyte Mp and to cause disease symptoms similar to those previously reported for the oomycete pathogen *P. palmivora* (Carella *et al.*, 2019). Rather than provoking the characteristic wilting phenotype observed on vascular plants, on Mp thalli the fungus provokes general disease symptoms such as tissue browning, maceration and cell death, which appear to be associated with the secretion of plant cell wall-degrading enzymes such as PGs. Importantly, we found that Fo can complete its infection cycle on Mp through the production of conidia and chlamydospores, which represents the main dispersal and survival structures of this pathogen during vascular wilt disease on angiosperms (Dean *et al.*, 2012).

Using isogenic deletion mutants of Fol4287, we established that infection of Mp requires a set of conserved pathogenicity factors including different MAPKs, transcription factors and cell wall remodelling enzymes. These genes are also required for pathogenicity of Fo on tomato (Di Pietro *et al.*, 2001; Caracuel *et al.*, 2005; Ruiz-Roldán *et al.*, 2015; Segorbe *et al.*, 2017) suggesting that core pathogenicity determinants contribute to fungal infection on evolutionarily distant plant lineages that diverged > 450 Ma (Delaux & Schornack, 2021).

The presence of broadly conserved pathogenicity mechanisms controlling invasive growth and colonisation of living plant tissue may explain why the endophytic isolate Fo47, which lacks host-specific virulence effectors and fails to cause wilting on

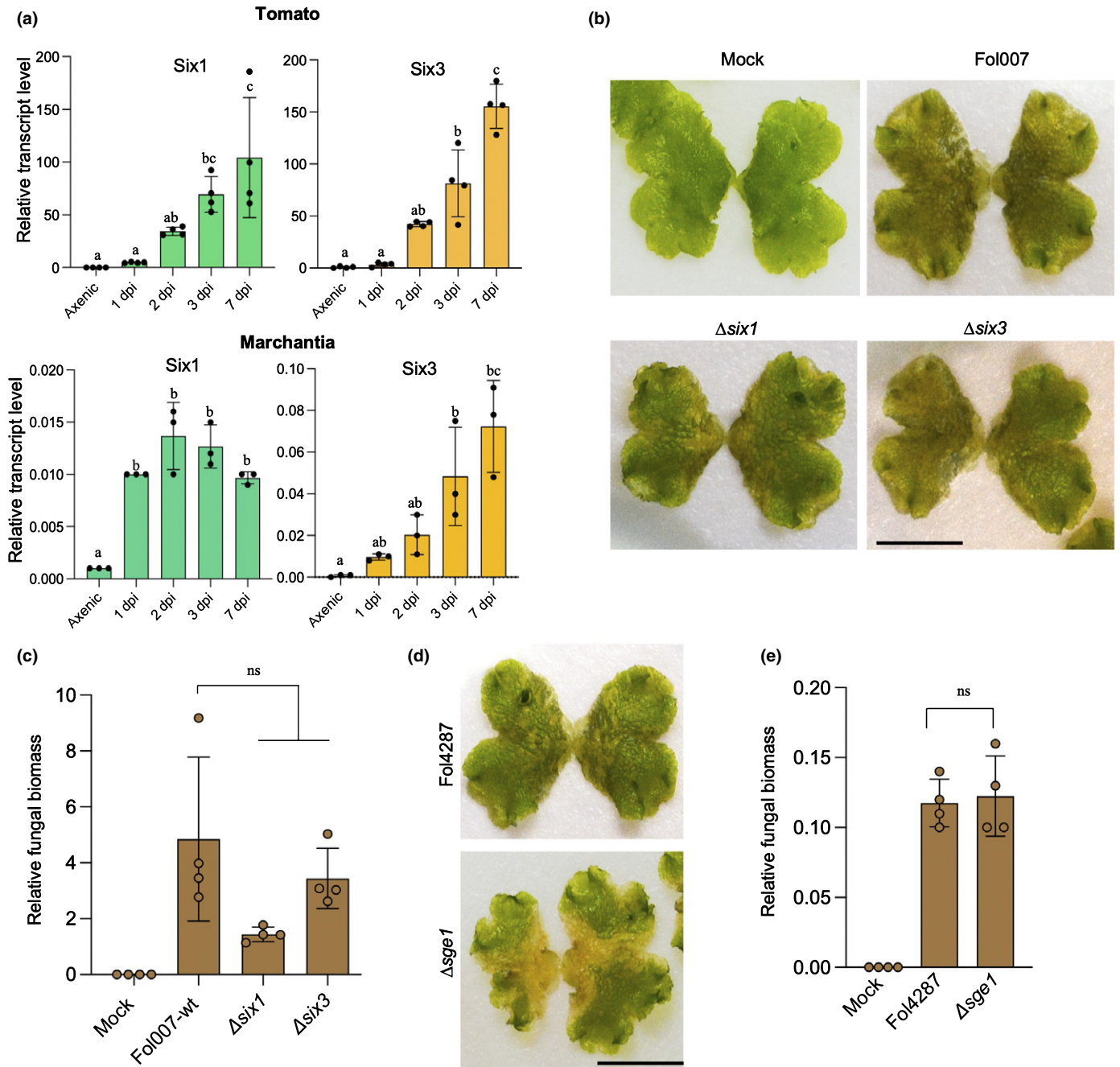


**Fig. 5** Tomato host-specific virulence effectors are largely dispensable for *Fusarium oxysporum* (Fo) infection on *Marchantia polymorpha*. (a) Transcript levels of the *six1* and *six3* genes were measured by reverse transcription quantitative polymerase chain reaction (RT-qPCR) of cDNA obtained from tomato roots (upper) or *M. polymorpha* Tak-1 plants (lower) at 1, 2, 3 and 7 d post inoculation (dpi) after dip inoculation with Fol4287, or from Fol4287 mycelium grown in liquid minimal medium (axenic). Transcript levels for each sample were calculated using the  $\Delta\Delta C_t$  method and normalised to those of the *Fo-ppi* gene. Error bars indicate standard deviation (SD) ( $n = 3$ ). Lowercase letters (a, b and c) indicate significant differences based on one-way analysis of variance (ANOVA) and Bonferroni's multiple comparison test. Note that upregulation of *six* effector genes *in planta* is approximately four orders of magnitude higher in the angiosperm tomato compared with the liverwort *Marchantia*. (b) Macroscopic images showing disease symptoms on *M. polymorpha* Tak-1 plants 6 dpi with  $10^5$  microconidia  $\text{ml}^{-1}$  of the wild-type strain (Fol007) or isogenic mutants in the *six1* or *six3* genes encoding lineage-specific (LS) virulence effectors secreted in the tomato xylem (SIX). Images are representative of three independent experiments. Bar, 1 cm. (c) Relative fungal biomass on *M. polymorpha* Tak-1 plants 6 dpi with  $10^5$  microconidia  $\text{ml}^{-1}$  of the Fol007 wild-type strain (Fol007-wt) or isogenic mutants in the *six1* or *six3* genes was measured using specific primers for the *Fo-actin* gene and normalised to the *MpEF1a* gene. Statistical significance vs Fol007-wt was calculated according to one-way ANOVA, Bonferroni's multiple comparison test (ns, nonsignificant,  $P > 0.05$ ). Error bars indicate SD;  $n = 4$ . (d) Macroscopic image showing disease symptoms on *M. polymorpha* Tak-1 plants 6 dpi with  $10^5$  microconidia  $\text{ml}^{-1}$  of the Fol4287 wild-type strain and the isogenic *sge1* mutant. Images are representative of three independent experiments. Bar, 1 cm. (e) Relative fungal biomass on *M. polymorpha* Tak-1 plants 6 dpi with  $10^5$  microconidia  $\text{ml}^{-1}$  of the Fol4287 wild-type strain, the isogenic *sge1* mutant or water (mock) was measured by real-time RT-qPCR using primers specific for the *Fo-actin* gene and normalised to the *M. polymorpha* *MpEF1a* gene. Statistical significance vs Fol4287 was calculated according to one-way ANOVA, Bonferroni's multiple comparison test (ns, nonsignificant,  $P > 0.05$ ). Error bars indicate SD ( $n = 4$ ).

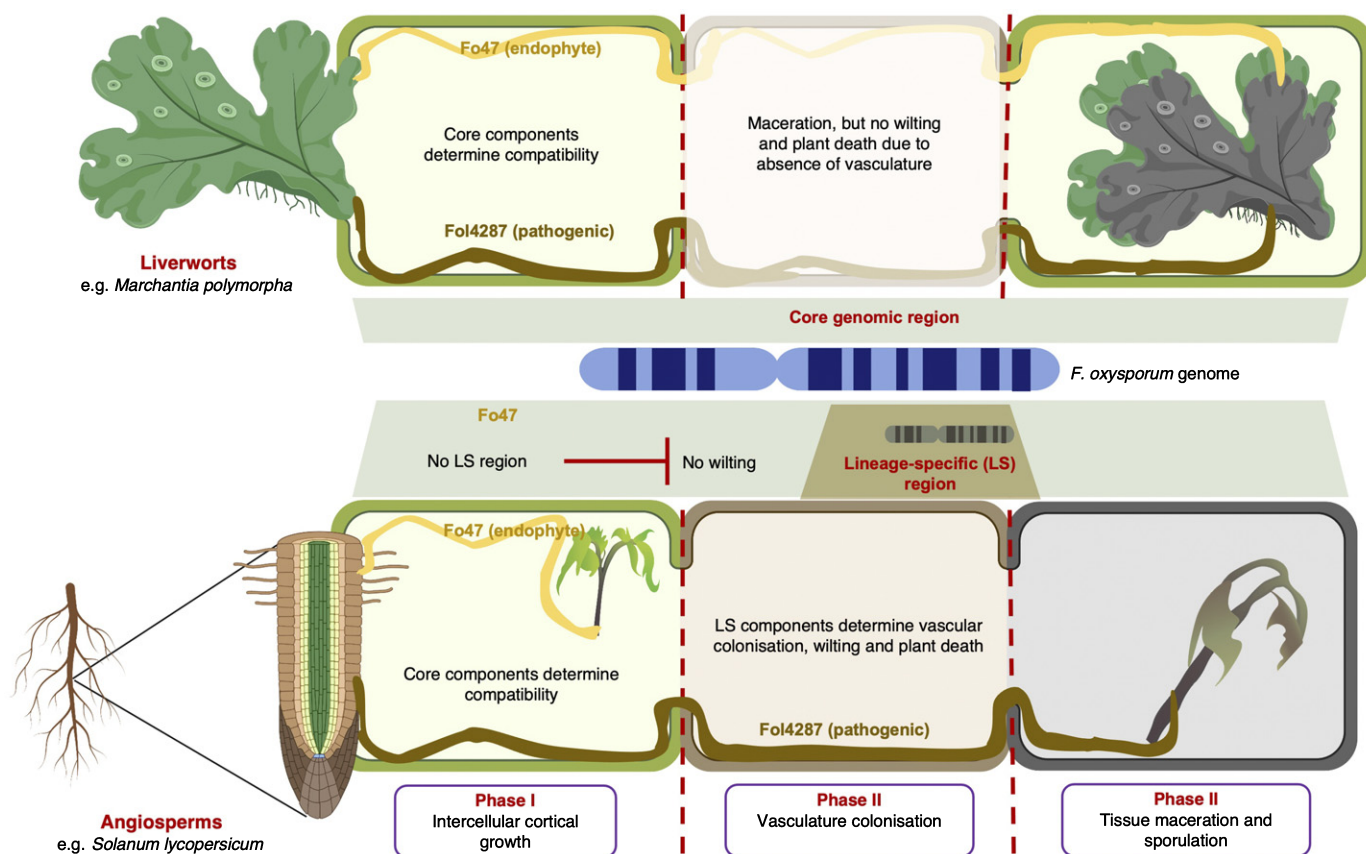


**Fig. 6** Distinct infection strategies of *Fusarium oxysporum* on vascular and nonvascular plants. Schematic diagram illustrating the infection strategies used by *F. oxysporum* during infection of a vascular (tomato) and a nonvascular plant host (*Marchantia polymorpha*). In the angiosperm host (lower panel), the infection cycle consists of three major phases: Phase I, asymptomatic intercellular growth in the root cortex; Phase II, entry into the xylem vessels and systemic colonisation of the host, eventually leading to plant death; and Phase III, extensive maceration of the moribund plant tissue and development of dispersal and resting structures (microconidia and macroconidia, chlamydospores). Phase II requires host-specific effectors encoded on lineage-specific (LS) genomic regions, whereas Phases I and III depend mainly on pathogenicity factors encoded on core regions. Infection of the bryophyte host *Marchantia* (upper panel) lacks Phase II due to the absence of a true vasculature and therefore depends exclusively on core pathogenicity factors. The model suggests that vasculature-mediated colonisation and wilting of the host plant by fungal pathogens evolved after the emergence of vascular land plants. We also propose that the core pathogenicity mechanisms are evolutionarily ancient and were present in fungal pathogens before the divergence of nonvascular and vascular plants. Parts of this figure were created using BIORENDER (<https://biorender.com/>).

angiosperm hosts (de Lamo & Takken, 2020), is able to induce similar disease symptoms on Mp as the pathogenic Fo strains even though the extent and timing of fungal and plant responses was somewhat different. This result suggests that infection of Fo on *Marchantia* involves principally Phases I (intercellular growth) and III (tissue maceration and sporulation) of the infection cycle (Fig. 6). Both phases require mainly core pathogenicity mechanisms, whereas Phase II (xylem colonisation), which is crucial for completion of the infection cycle on angiosperms, depends critically on effectors encoded on LS regions. In line with this, we found that the *six1* and *six3* genes, which are highly upregulated in xylem and contribute to virulence on tomato, are largely dispensable for infection of Mp. We speculate that this differential role can be ascribed to the lack of a true vasculature in Mp, which results in the absence of Phase II of the disease cycle on angiosperms involving colonisation of the xylem vessels (Fig. 6). Absence of wilting in *Marchantia* is further supported by the finding that, in spite of the severe disease symptoms observed at the centre of the thallus, all infected plants survived Fo infection

and eventually resumed apical growth at the meristematic tissue. Interestingly, the presence of Fo hyphae in the asymptomatic regions adjacent to the macerated area suggest that Fo can systematically colonise the thallus, exhibiting initially an endophytic lifestyle.

Interestingly, the partial upregulation of the *six1* gene on Mp and the reduced fungal burden of the *six1* mutant suggested that this LS effector may play at least an accessory role during infection of this nonvascular plant. Although *six1* was originally thought to be expressed exclusively in the tomato xylem, it was later found to be upregulated also in undifferentiated cell cultures of tomato and other plant species such as *Nicotiana*, indicating that its induction does not depend on root-specific features (van der Does *et al.*, 2008). Moreover, in addition to the tomato pathogenic f.sp. *lycopersici*, other ff.spp. of Fo also carry *six1* homologues, including *cubense* (banana), *pisi* (pea), *conglutinans* (crucifers) or *melonis* (melon) (van Dam *et al.*, 2016). Collectively, this suggests that this LS effector has evolved to fulfil general virulence functions during growth of Fo on living plant

tissue, including the nonvascular host Mp. Conversely, we found that another LS effector, *six3*, as well as the transcriptional regulator Sge1, which is encoded by the core genome of Fo, do not contribute significantly to infection on Mp thalli. Interestingly, Sge1 is required for expression of LS virulence effectors and pathogenicity on tomato, but not for root penetration and colonisation (Michielse *et al.*, 2009), suggesting that it contributes mainly to infection Phase II in the xylem and providing a possible explanation for its dispensability on the nonvascular host Mp. Future studies will be required to precisely define the transcriptional co-ordination of virulence factors from core and LS regions and their role during infection of Mp.

An important goal in Evo-MPMI is to understand how plant immunity has evolved. We observed a marked growth inhibition of Mp upon exposure to Fo mycelial extracts, mirroring the results obtained previously with the bacterial pathogen *P. syringae* (Gimenez-Ibanez *et al.*, 2019). Moreover, treatment with chito-hexaose, an oligosaccharide derived from chitin, which is a major component of fungal cell walls, triggered rapid upregulation of defence-related marker genes in Mp, suggesting that this plant can sense fungal invaders and mount a defence response. Chitin receptors in plants have been studied extensively (Shinya *et al.*, 2015), and Mp was shown to possess an orthologue of CERK1, containing a lysine motif (LysM)-RK that mediates perception of peptidoglycans (PGNs) and chitin in angiosperms (Boutrot & Zipfel, 2017). While further experiments are needed to elucidate how chito-hexaose is perceived by Mp, our findings suggest that Mp can sense PAMPs from different Fo strains. This suggestion is further supported by the observed upregulation of the PAMP responsive genes *WRKY22* and *CML42* (Navarro *et al.*, 2004; Gimenez-Ibanez *et al.*, 2019) or the PR protein genes *PR4* and *PR9* upon treatment with chito-hexaose, which can act as fungal PAMP. Moreover, upregulation of syntaxin Mp *SYP13B*, which localises around the microbial infection structure (Carella *et al.*, 2019), the flavonoid biosynthesis components *PAL* and *Myb14*, as well as *PR4* and *PR9*, was detected during natural Fo infection. As the Mp genome contains only one-third of the receptor kinases found in *A. thaliana* (Bowman *et al.*, 2017), the availability of a rapid and robust assay for a PTI-like response to Fo will facilitate the identification of novel fungal PAMPs and cognate PRRs that trigger immune activation in bryophytes.

In summary, our work on this newly established pathogen–host system reveals that Fo, a root-infecting vascular wilt fungus in angiosperms has the capacity to cause disease in nonvascular plants. Markedly, two Fo strains with opposed lifestyles – pathogenic vs endophytic – both behave as pathogens in Mp, most probable because they share a common set of core pathogenicity factors required for infection of both vascular and nonvascular plants. Host-specific or xylem-specific virulence factors that are crucial for infection in angiosperm hosts appear to play a minor role on Mp. This is consistent with the idea that specialised virulence effectors, which are mostly encoded on LS regions, were acquired by vascular wilt pathogens after the emergence of vascular plants. Therefore, our study provides new insights into the core compatibility mechanisms that mediate plant associations in vascular wilt pathogens. Collectively, these findings further highlight the potential of the

*Marchantia* infection model to advance our understanding of the evolution of plant–microbe interactions.


## Acknowledgements


AR and MS acknowledge funding from the European Union's Horizon 2020 research and innovation programme under the Marie Skłodowska-Curie grant agreement nos. 750669 and 797256. ADP acknowledges support from the Spanish Ministry of Science and Innovation (MICINN, grant no. PID2019-108045RB-I00) and Junta de Andalucía (grant no. P20\_00179). AR acknowledges funding from a Juan de la Cierva Incorporación grant from MICINN (IJC2018-038468-I). Work in the RS laboratory was funded by the Spanish Ministry of Science and Innovation grant no. PID2019-107012RB-I00/AEI/10.13039/501100011033. SGI is funded by a Ramon y Cajal Fellowship RYC2019-026396-I, the CSIC grant no. 20212AT006 and the Spanish Ministry of Science and Innovation grant for young investigators RTI2018-094526-J-I00. We are grateful to Martijn Rep, University of Amsterdam for kindly providing the *F. oxysporum* Fol007,  $\Delta$ *six1*,  $\Delta$ *six3* and  $\Delta$ *sge1* strains and to David Turrà, University of Naples for contributing the clover-expressing Fo strains. Funding for open access of this article was supported by Universidad de Córdoba-CBUA. The authors declare no conflict of interest.


## Author contributions


AR, SGI, RS and ADP conceptualised and designed the research. AR, SGI, MS and BZ conducted all experiments. AR, SGI, MS and BZ, performed the data analysis. AR and ADP wrote the manuscript with input from all co-authors. All authors reviewed and approved the manuscript.


## ORCID


Antonio Di Pietro  <https://orcid.org/0000-0001-5930-5763>

Selena Gimenez Ibanez  <https://orcid.org/0000-0002-5453-8565>

Amey Redkar  <https://orcid.org/0000-0001-5171-8061>

Mugdha Sabale  <https://orcid.org/0000-0001-7464-6996>

Roberto Solano  <https://orcid.org/0000-0001-5459-2417>

Bernd Zechmann  <https://orcid.org/0000-0002-7702-2588>

## Data availability

The data and any generated material that support the findings of this study are available from the corresponding author upon reasonable request.

## References

- Alabouvette C. 1986. *Fusarium*-wilt suppressive soils from the châteaurenard region: review of a 10-year study. *Agronomie* 6: 273–284.
- Ali S, Ganai BA, Kamili AN, Bhat AA, Mir ZA, Bhat JA, Tyagi A, Islam ST, Mushtaq M, Yadav P *et al.* 2018. Pathogenesis-related proteins and peptides as promising tools for engineering plants with multiple stress tolerance. *Microbiological Research* 212–213: 29–37.

- Bajar BT, Wang ES, Lam AJ, Kim BB, Jacobs CL, Howe ES, Davidson MW, Lin MZ, Chu J. 2016. Improving brightness and photostability of green and red fluorescent proteins for live cell imaging and FRET reporting. *Scientific Reports* 6: 20889.
- Boller T, Felix G. 2009. A renaissance of elicitors: perception of microbe-associated molecular patterns and danger signals by pattern-recognition receptors. *Annual Review of Plant Biology* 60: 379–406.
- Bonfante P, Genre A. 2010. Mechanisms underlying beneficial plant–fungus interactions in mycorrhizal symbiosis. *Nature Communications* 1: 48.
- Boutrot F, Zipfel C. 2017. Function, discovery, and exploitation of plant pattern recognition receptors for broad-spectrum disease resistance. *Annual Review of Phytopathology* 55: 257–286.
- Bowman JL, Kohchi T, Yamato KT, Jenkins J, Shu S, Ishizaki K, Yamaoka S, Nishihama R, Nakamura Y, Berger F *et al.* 2017. Insights into land plant evolution garnered from the *Marchantia polymorpha* Genome. *Cell* 171: 287–304.e215.
- Bravo Ruiz G, Di Pietro A, Roncero MIG. 2016. Combined action of the major secreted exo- and endopolygalacturonases is required for full virulence of *Fusarium oxysporum*. *Molecular Plant Pathology* 17: 339–353.
- Caracul Z, Martínez-Rocha AL, Di Pietro A, Madrid MP, Roncero MIG. 2005. *Fusarium oxysporum gas1* encodes a putative  $\beta$ -1,3-glucanotransferase required for virulence on tomato plants. *Molecular Plant–Microbe Interactions* 18: 1140–1147.
- Carella P, Gogleva A, Tomaselli M, Alfs C, Schornack S. 2018. *Phytophthora palmivora* establishes tissue-specific intracellular infection structures in the earliest divergent land plant lineage. *Proceedings of the National Academy of Sciences, USA* 115: E3846–E3855.
- Carella P, Gogleva A, Hoey DJ, Bridgen AJ, Stolze SC, Nakagami H, Schornack S. 2019. Conserved biochemical defenses underpin host responses to oomycete infection in an early-divergent land plant lineage. *Current Biology* 29: 2282–2294.e5.
- van Dam P, Fokkens L, Schmidt SM, Linmans JHJ, Kistler HC, Ma L-J, Rep M. 2016. Effector profiles distinguish formae speciales of *Fusarium oxysporum*. *Environmental Microbiology* 18: 4087–4102.
- Dean R, Van kan JAL, Pretorius ZA, Hammond-kosack KE, Di pietro A, Spanu PD, Rudd JJ, Dickman M, Kahmann R, Ellis J *et al.* 2012. The top 10 fungal pathogens in molecular plant pathology. *Molecular Plant Pathology* 13: 414–430.
- Delulio GA, Guo L, Zhang Y, Goldberg JM, Kistler HC, Ma L-J. 2018. Kinome expansion in the *Fusarium oxysporum* species complex driven by accessory chromosomes. *mSphere* 3: e00231-18.
- Delaux P-M, Schornack S. 2021. Plant evolution driven by interactions with symbiotic and pathogenic microbes. *Science* 371: eaba6605.
- Di Pietro A, García-Maceira FI, Męglec E, Roncero MIG. 2001. A MAP kinase of the vascular wilt fungus *Fusarium oxysporum* is essential for root penetration and pathogenesis. *Molecular Microbiology* 39: 1140–1152.
- Di Pietro A, Roncero MIG. 1998. Cloning, expression, and role in pathogenicity of pg1 encoding the major extracellular endopolygalacturonase of the vascular wilt pathogen *Fusarium oxysporum*. *Molecular Plant–Microbe Interactions* 11: 91–98.
- van der Does HC, Duyvesteijn RGE, Goltstein PM, van Schie CCN, Manders EMM, Cornelissen BJC, Rep M. 2008. Expression of effector gene SIX1 of *Fusarium oxysporum* requires living plant cells. *Fungal Genetics and Biology* 45: 1257–1264.
- van der Does HC, Rep M. 2017. Adaptation to the host environment by plant-pathogenic fungi. *Annual Review of Phytopathology* 55: 427–450.
- García-Maceira FI, Di Pietro A, Huertas-González MD, Ruiz-Roldán MC, Roncero MIG. 2001. Molecular characterization of an endopolygalacturonase from *Fusarium oxysporum* expressed during early stages of infection. *Applied and Environmental Microbiology* 67: 2191–2196.
- Gimenez-Ibanez S, Zamarreño AM, García-Mina JM, Solano R. 2019. An evolutionarily ancient immune system governs the interactions between *Pseudomonas syringae* and an early-diverging land plant lineage. *Current Biology* 29: 2270–2281.e2274.
- Gordon TR. 2017. *Fusarium oxysporum* and the *Fusarium* Wilt Syndrome. *Annual Review of Phytopathology* 55: 23–39.
- Houterman PM, Ma L, Van Ooijen G, De Vroomen MJ, Cornelissen BJC, Takken FLW, Rep M. 2009. The effector protein Avr2 of the xylem-colonizing fungus *Fusarium oxysporum* activates the tomato resistance protein I-2 intracellularly. *The Plant Journal* 58: 970–978.
- Ishizaki K, Chiyoda S, Yamato KT, Kohchi T. 2008. Agrobacterium-mediated transformation of the haploid liverwort *Marchantia polymorpha* L., an emerging model for plant biology. *Plant and Cell Physiology* 49: 1084–1091.
- Jones JDG, Dangl JL. 2006. The plant immune system. *Nature* 444: 323–329.
- Jones K, Kim DW, Park JS, Khang CH. 2016. Live-cell fluorescence imaging to investigate the dynamics of plant cell death during infection by the rice blast fungus *Magnaporthe oryzae*. *BMC Plant Biology* 16: 69.
- de Jonge R, Bolton MD, Thomma BPHJ. 2011. How filamentous pathogens co-opt plants: the ins and outs of fungal effectors. *Current Opinion in Plant Biology* 14: 400–406.
- Kubo H, Nozawa S, Hiwatashi T, Kondou Y, Nakabayashi R, Mori T, Saito K, Takanashi K, Kohchi T, Ishizaki K. 2018. Biosynthesis of riccionidins and marchantins is regulated by R2R3-MYB transcription factors in *Marchantia polymorpha*. *Journal of Plant Research* 131: 849–864.
- de Lamo FJ, Takken FLW. 2020. Biocontrol by *Fusarium oxysporum* using endophyte-mediated resistance. *Frontiers in Plant Science* 11: 37.
- Livak KJ, Schmittgen TD. 2001. Analysis of relative gene expression data using real-time quantitative PCR and the  $2^{-\Delta\Delta CT}$  method. *Methods* 25: 402–408.
- Lockhart J. 2015. The elegant simplicity of the Liverwort *Marchantia polymorpha*. *Plant Cell* 27: 1565.
- López-Berges MS, Rispail N, Prados-Rosales RC, Di Pietro A. 2010. A nitrogen response pathway regulates virulence functions in *Fusarium oxysporum* via the protein kinase TOR and the bZIP protein MeaB. *Plant Cell* 22: 2459–2475.
- Ma L-J, van der Does HC, Borkovich KA, Coleman JJ, Daboussi M-J, Di Pietro A, Dufresne M, Freitag M, Grabherr M, Henrissat B *et al.* 2010. Comparative genomics reveals mobile pathogenicity chromosomes in *Fusarium*. *Nature* 464: 367–373.
- Masachus S, Segorbe D, Turrà D, Leon-Ruiz M, Fürst U, El Ghalid M, Leonard G, López-Berges MS, Richards TA, Felix G *et al.* 2016. A fungal pathogen secretes plant alkalizing peptides to increase infection. *Nature Microbiology* 1: 16043.
- Matsui H, Iwakawa H, Hyon G-S, Yotsui I, Katou S, Monte I, Nishihama R, Franzen R, Solano R, Nakagami H. 2019. Isolation of natural fungal pathogens from *Marchantia polymorpha* reveals antagonism between salicylic acid and jasmonate during liverwort-fungus interactions. *Plant and Cell Physiology* 61: 265–275.
- Matthaeus WJ, Schmidt J, White JD, Zechmann B. 2020. Novel perspectives on stomatal impressions: rapid and non-invasive surface characterization of plant leaves by scanning electron microscopy. *PLoS ONE* 15: e0238589.
- Michiels CB, Rep M. 2009. Pathogen profile update: *Fusarium oxysporum*. *Molecular Plant Pathology* 10: 311–324.
- Michiels CB, van Wijk R, Reijnen L, Manders EMM, Boas S, Olivain C, Alabouvette C, Rep M. 2009. The nuclear protein Sge1 of *Fusarium oxysporum* is required for parasitic growth. *PLoS Pathogens* 5: e1000637.
- Navarro L, Zipfel C, Rowland O, Keller I, Robatzek S, Boller T, Jones JDG. 2004. The transcriptional innate immune response to flg22. Interplay and overlap with Avr gene-dependent defense responses and bacterial pathogenesis. *Plant Physiology* 135: 1113–1128.
- Nelson JM, Hauser DA, Hinson R, Shaw AJ. 2018. A novel experimental system using the liverwort *Marchantia polymorpha* and its fungal endophytes reveals diverse and context-dependent effects. *New Phytologist* 218: 1217–1232.
- Nelson JM, Shaw AJ. 2019. Exploring the natural microbiome of the model liverwort: fungal endophyte diversity in *Marchantia polymorpha* L. *Symbiosis* 78: 45–59.
- Pérez-Nadales E, Di Pietro A. 2011. The membrane Mucin Msb2 regulates invasive growth and plant infection in *Fusarium oxysporum*. *Plant Cell* 23: 1171–1185.
- Presti LL, Lanver D, Schweizer G, Tanaka S, Liang L, Tollot M, Zuccaro A, Reissmann S, Kahmann R. 2015. Fungal effectors and plant susceptibility. *Annual Review of Plant Biology* 66: 513–545.
- Redkar A, Sabale M, Schudoma C, Zechmann B, Gupta YK, López-Berges MS, Venturini G, Gimenez Ibanez S, Turrà D, Solano R *et al.* 2021. Conserved secreted effectors determine endophytic growth and multi-host plant

- compatibility in a vascular wilt fungus. *bioRxiv*. doi: 10.1101/2021.08.29.457830.
- Rep M, Van Der Does HC, Meijer M, Van Wijk R, Houterman PM, Dekker HL, De Koster CG, Cornelissen BJC. 2004. A small, cysteine-rich protein secreted by *Fusarium oxysporum* during colonization of xylem vessels is required for I-3-mediated resistance in tomato. *Molecular Microbiology* 53: 1373–1383.
- Ruiz-Roldán C, Pareja-Jaime Y, González-Reyes JA, Roncero MIG 2015. The transcription factor Con7-1 is a master regulator of morphogenesis and virulence in *Fusarium oxysporum*. *Molecular Plant–Microbe Interactions* 28: 55–68.
- Ryder LS, Talbot NJ. 2015. Regulation of appressorium development in pathogenic fungi. *Current Opinion in Plant Biology* 26: 8–13.
- Saruyama N, Sakakura Y, Asano T, Nishiuchi T, Sasamoto H, Kodama H. 2013. Quantification of metabolic activity of cultured plant cells by vital staining with fluorescein diacetate. *Analytical Biochemistry* 441: 58–62.
- Segorbe D, Di Pietro A, Pérez-Nadales E, Turrà D. 2017. Three *Fusarium oxysporum* mitogen-activated protein kinases (MAPKs) have distinct and complementary roles in stress adaptation and cross-kingdom pathogenicity. *Molecular Plant Pathology* 18: 912–924.
- Shinya T, Nakagawa T, Kaku H, Shibuya N. 2015. Chitin-mediated plant–fungal interactions: catching, hiding and handshaking. *Current Opinion in Plant Biology* 26: 64–71.
- Tintor N, Paauw M, Rep M, Takken FLW. 2020. The root-invading pathogen *Fusarium oxysporum* targets pattern-triggered immunity using both cytoplasmic and apoplastic effectors. *New Phytologist* 227: 1479–1492.
- Torres AM, Weeden NF, Martín A. 1993. Linkage among isozyme, RFLP and RAPD markers in *Vicia faba*. *Theoretical and Applied Genetics* 85: 937–945.
- Turrà D, El Ghalid M, Rossi F, Di Pietro A. 2015. Fungal pathogen uses sex pheromone receptor for chemotropic sensing of host plant signals. *Nature* 527: 521–524.
- Turrà D, Segorbe D, Pietro AD. 2014. Protein kinases in plant–pathogenic fungi: conserved regulators of infection. *Annual Review of Phytopathology* 52: 267–288.
- Upton JL, Zess EK, Bialas A, Wu C-H, Kamoun S. 2018. The coming of age of EvoMPMI: evolutionary molecular plant–microbe interactions across multiple timescales. *Current Opinion in Plant Biology* 44: 108–116.
- Vlaardingerbroek I, Beerens B, Schmidt SM, Cornelissen BJC, Rep M. 2016. Dispensable chromosomes in *Fusarium oxysporum* f. sp. *lycopersici*. *Molecular Plant Pathology* 17: 1455–1466.
- Wang B, Yu H, Jia Y, Dong Q, Steinberg C, Alabouvette C, Edel-Hermann V, Kistler HC, Ye K, Ma L-J *et al.* 2020. Chromosome-scale genome assembly of *Fusarium oxysporum* strain Fo47, a fungal endophyte and biocontrol agent. *Molecular Plant–Microbe Interactions* 33: 1108–1111.
- Weiberg A, Wang M, Bellinger M, Jin H. 2014. Small RNAs: a new paradigm in plant–microbe interactions. *Annual Review of Phytopathology* 52: 495–516.
- Xue J-Y, Wang Y, Wu P, Wang Q, Yang L-T, Pan X-H, Wang B, Chen J-Q. 2012. A primary survey on bryophyte species reveals two novel classes of nucleotide-binding site (NBS) genes. *PLoS ONE* 7: e36700.
- Yadeta K, Thomma B. 2013. The xylem as battleground for plant hosts and vascular wilt pathogens. *Frontiers in Plant Science* 4: 97.

## Supporting Information

Additional Supporting Information may be found online in the Supporting Information section at the end of the article.

**Fig. S1** Effect of inoculum concentration on disease progression during infection with different Fo isolates on thalli of *Marchantia polymorpha*.

**Fig. S2** Fo causes tissue maceration mainly at the centre of the *Marchantia polymorpha* thallus and colonises apical notches endophytically.

**Fig. S3** Different inoculation methods lead to similar disease symptoms on *Marchantia polymorpha* and Fo preference to colonise the thalloid tissue.

**Fig. S4** Early infection by Fo occurs on living *Marchantia polymorpha* cells.

**Fig. S5** Production of Fo survival structures on macerated *Marchantia polymorpha* tissue.

**Fig. S6** *Marchantia polymorpha* responds to pathogen-associated molecular pattern (PAMP) signatures from different Fo strains and to purified chitohexose.

**Fig. S7** Role of core pathogenicity genes in colony development and virulence of Fo4287 on tomato plants.

**Fig. S8** Extent of cell death in *Marchantiapolymorpha* thalli inoculated with isogenic mutants lacking Fo core pathogenicity determinants.

**Fig. S9** Lineage-specific virulence effectors are largely dispensable for Fo infection on *Marchantia polymorpha*.

**Table S1** *Fusarium oxysporum* strains used in the study.

**Table S2** Oligonucleotides used in the study.

Please note: Wiley Blackwell are not responsible for the content or functionality of any Supporting Information supplied by the authors. Any queries (other than missing material) should be directed to the *New Phytologist* Central Office.